Complex Bifurcation of Arnol'd Tongues Generated in Three-Coupled Delayed Logistic Maps

Daiki Ogusu, Shuya Hidaka, Naohiko Inaba, Munehisa Sekikawa and Tetsuro Endo

Abstract This study investigates quasi-periodic bifurcations and Arnol'd resonance webs generated in a three-coupled delayed logistic map. Complex bifurcation structure is generated when a conventional Arnol'd tongue transits to a higher-dimensional Arnol'd tongue. We discovered that, at least, two periodic attractors coexist in the conventional Arnol'd tongue which can bifurcate to two one-tori via doubly-folded Neimark–Sacker bifurcation.

1 Summary

The partial and complete synchronization of three or higher frequency quasi-periodic oscillations has recently been studied extensively [1]. Vitolo et al. clarified that two types of bifurcation routes from a two-dimensional torus to a three-dimensional torus exists [2]. One is a quasi-periodic Hopf (QH) bifurcation, and the other is a quasi-periodic saddle-node (QSN) bifurcation. The Arnol'd resonance web is a phenomenon that was discovered and defined by Broer et al. [1] in the numerical

D. Ogusu (✉) · S. Hidaka · T. Endo
Department of Electronics and Bioinformatics, Meiji University, Kawasaki 214-8571, Japan
e-mail: ce51011@meiji.ac.jp

S. Hidaka
e-mail: ce41083@meiji.ac.jp

T. Endo
e-mail: endoh@meiji.ac.jp

N. Inaba
Organization for the Strategic Coordination of Research and Intellectual Property, Meiji University, Kawasaki 214-8571, Japan
e-mail: naohiko@yomogi.jp

M. Sekikawa
Department of Mechanical and Intelligent Engineering, Utsunomiya University, Utsunomiya 321-8585, Japan
e-mail: sekikawa@cc.utsunomiya-u.ac.jp

G. Mantica et al. (eds.), *Emergent Complexity from Nonlinearity, in Physics, Engineering and the Life Sciences*, Springer Proceedings in Physics 191,
DOI 10.1007/978-3-319-47810-4_2

analysis of a map, where regions generating invariant closed curves (ICCs) corresponding to two-dimensional tori in vector fields extend in many directions in the invariant torus-generating region like a web.

One of the major concerns in this field is the problem how a conventional Arnol'd tongue transits to a higher dimensional Arnol'd tongue near QH bifurcation curves. Takens and Wagener provided a bifurcation diagram near the parameter regions [3], and Kuznetsov and Meijer conducted Lypunov analysis [4]. The simplest one may be the transition from a conventional Arnol'd tongue to a two-dimensional torus-Arnol'd tongue via Neimark–Sacker bifurcation [5]. More complex one was reported by Broer et al. [6].

In this study, we conduct a Lyapunov analysis for a three-coupled delayed logistic map expressed by the following form:

$$
\begin{aligned}
F(x_n, y_n, z_n, & \; x_{n+1} = y_n, \\
w_n, u_n, v_n)^\top : & \; y_{n+1} = B_1 y_n(1 - x_n) + \varepsilon_1 w_n + \varepsilon_2 v_n, \\
& \; z_{n+1} = w_n, \\
& \; w_{n+1} = B_2 w_n(1 - z_n) + \varepsilon_3 v_n + \varepsilon_4 y_n, \\
& \; u_{n+1} = v_n, \\
& \; v_{n+1} = B_3 v_n(1 - u_n) + \varepsilon_5 y_n + \varepsilon_6 w_n.
\end{aligned} \tag{1}
$$

We classify the phenomena in Fig. 1. If the largest Lyapunov exponent is negative, the attractor is defined as periodic, and is denoted by orange in the Lyapunov diagrams shown later. If the largest Lyapunov exponent is positive, the attractor is defined as chaotic, and is denoted by red in the diagram. Because the objective dynamics is discrete, the attractor is torus if the largest Lyapunov exponent λ_1 equals zero. If only λ_1 is zero, the attractor is called invariant one-torus (IT_1) corresponding to a two-torus in vector fields, which is denoted by blue in the diagrams. The three-torus and four-torus abbreviated as IT_2 and IT_3, respectively are defined as in Fig. 1.

We use such abbreviation as shown in Fig. 2 for the several types of bifurcations. Throughout this study, a Neimark–Sacker bifurcation is abbreviated by NS, a saddle-node bifurcation is abbreviated by SN, a quasi-periodic Hopf bifurcation from IT_1 to IT_2 is abbreviated by QH, and a quasi-periodic saddle-node bifurcation from IT_1 to IT_2 is denoted by QSN. A quasi-periodic Hopf bifurcation from IT_2 to IT_3 is denoted by QH_2 and a quasi-periodic saddle-node bifurcation from IT_2 to IT_3 is denoted by QSN_2.

Map	Vector fields	Lyapunov exponents	Color
Periodic (IT_0)	Periodic	$\lambda_1 < 0$	orange
Invariant one-torus (IT_1)	Two-torus	$\lambda_1 = 0, \lambda_2 < 0$	blue
Invariant two-torus (IT_2)	Three-torus	$\lambda_1 = \lambda_2 = 0, \lambda_3 < 0$	black
Invariant three-torus (IT_3)	Four-torus	$\lambda_1 = \lambda_2 = \lambda_3 = 0, \lambda_4 < 0$	dark green
Chaos	Chaos	$\lambda_1 > 0$	red

Fig. 1 Correspondence of terminologies and colors

Bifurcations	Abbreviated terms
Neimark-Sacker bifurcation from IT_0(periodic) to IT_1	NS
Saddle-node bifurcation from IT_0(periodic) to IT_1	SN
Quasi-periodic Hopf bifurcation from IT_1 to IT_2	QH
Quasi-periodic saddle-node bifurcation from IT_1 to IT_2	QSN
Quasi-periodic Hopf bifurcation from IT_2 to IT_3	QH_2
Quasi-periodic saddle-node bifurcation from IT_2 to IT_3	QSN_2

Fig. 2 Abbreviations for the several types of bifurcations

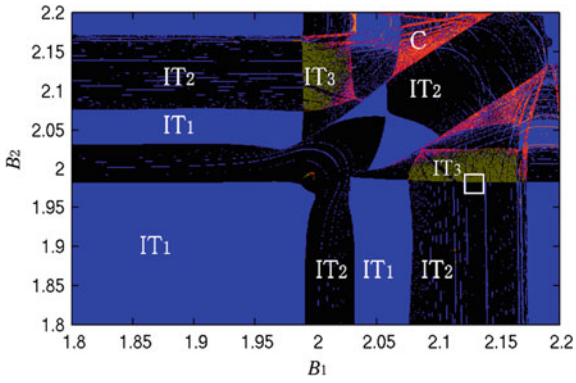

Fig. 3 Global view of Lyapunov diagram of (1) for $\varepsilon_1 = 0.01$, $\varepsilon_2 = 0.002$, $\varepsilon_3 = 0.001$, $\varepsilon_4 = 0.02$, $\varepsilon_5 = 0.01$, $\varepsilon_6 = 0.01$, and $B_3 = 2.05$

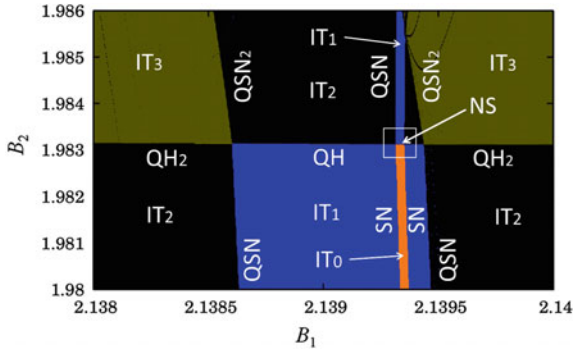

Fig. 4 Magnified view of the *square* region of the Lyapunov diagram in Fig. 3. Parameters are the same as those in Fig. 3

Figure 3 shows a global view of Lyapunov diagram of the three coupled delayed logistic maps shown in (1). In the figure, horizontal and vertical axes are parameters B_1 and B_2, respectively. The Lyapunov exponents are calculated using the procedure presented by Shimada and Nagashima [7]. The region marked IT_1 is the region where an invariant one-torus is generated. In the same manner, IT_2, IT_3, and C denote the regions where an invariant two-torus, an invariant three-torus, and chaos are generated, respectively. We pay attention to the square region.

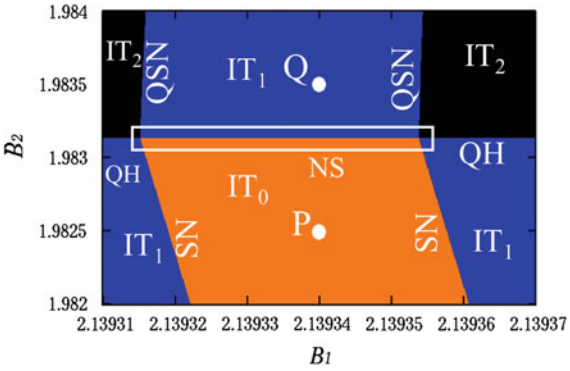

Fig. 5 Further magnified view of the *square* region of the Lyapunov diagram in Fig. 4. Parameters are the same as those in Fig. 3. The *squared* region is used after

Figure 4 shows the magnified view of the square region in Fig. 3. As seen in the figure, the IT_1 Arnol'd tongue transits to the IT_2 Arnol'd tongue via QH or QSN. We focus on bifurcation structure where a conventional (IT_0) Arnol'd tongue bifurcates to invariant one-torus (IT_1) Arnol'd tongue through a Neimark–Sacker bifurcation. At first glance, this bifurcation structure appears to be a simple transition. However, the bifurcation structure is complex according to our numerical results.

Figure 5 shows a further magnified view of the square region of the Lyapunov diagram in Fig. 4. Our concern is what kind of bifurcation occurs when a parameter is moved from P to Q across NS. Figure 6a shows the periodic attractors obtained at the point marked $P : (B_1, B_2) = (2.13934, 1.9825)$ in Fig. 5. Figure 6b shows a magnified view of the square region in Fig. 6a. Note that two attractors coexist in the IT_0 Arnol'd tongue at P. One is denoted as red crosses and the other is denoted as green crosses, each of which consists of a periodic attractor with a period of 93. Figure 7 shows coexisting two invariant one-tori (IT_1) obtained at $Q : (B_1, B_2) = (2.13934, 1.9835)$. The coexisting periodic attractors at P bifurcate to two invariant one-tori through a Neimark–Sacker bifurcation. To the best of our knowledge, this is a novel bifurcation structure. The reason is explained below.

Figure 8a shows a doubly-folded Neimark–Sacker bifurcation curve obtained by magnifying the squared region in Fig. 5. Figure 8b shows the schematic in Fig. 8a. The skyblue curves denote Neimark–Sacker bifurcation of the stable periodic points, and the brown curves denote Neimark–Sacker bifurcation of the unstable periodic points. Note that the bifurcation curves of the unstable periodic points do not affect bifurcation of the attractors. There are four stable SN bifurcation lines on the both side of the stable and unstable NS bifurcation curves. They are tangent to the NS bifurcation curves at four points at which codimension-two bifurcation occurs. Note that the Neimark–Sacker bifurcation curve is doubly twisted. This bifurcation structure explains the coexisting periodic solutions (IT_0) and coexisting invariant one-tori (IT_1). In the region below the stable NS curves, stable coexisting two periodic solutions are observed, and they bifurcate to invariant one-tori via two Neimark–Sacker bifurcations. Since Neimark–Sacker bifurcation is doubly folded, existence of four codimension-two bifurcation points are naturally explained.

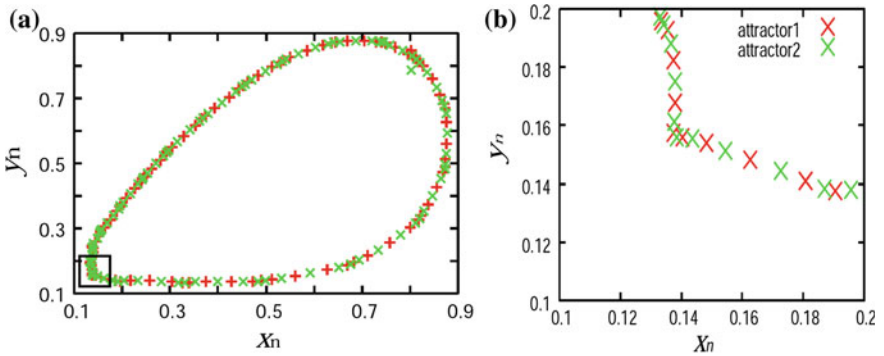

Fig. 6 Coexisting two periodic attractors with period of 93 obtained at a *point* marked $P : (B_1, B_2) = (2.13934, 1.9825)$ in Fig. 5. Parameters are given in Fig. 3. **a** Whole view **b** magnified view of the *squared* region

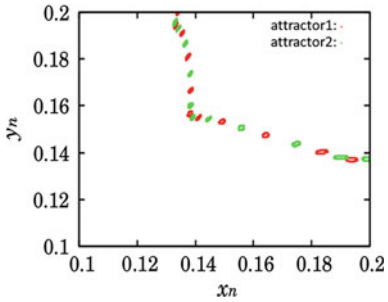

Fig. 7 Magnified diagram of a part of the coexisting two invariant one-tori for $Q : (B_1, B_2) = (2.13934, 1.9835)$ after NS bifurcation

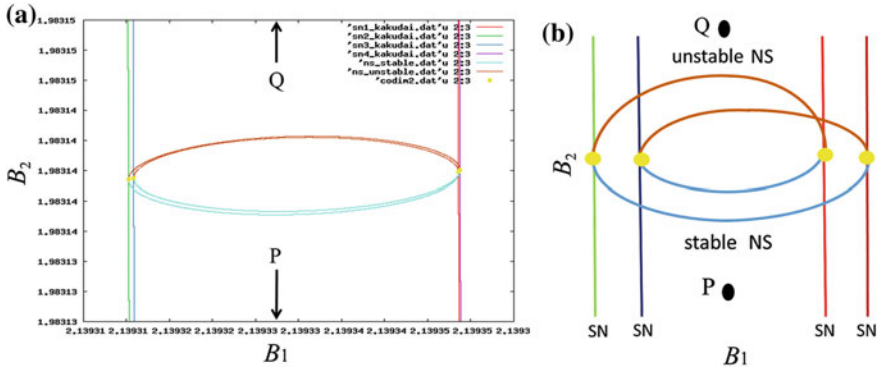

Fig. 8 A doubly-folded Neimark–Sacker bifurcation curve. Two *skyblue* curves present the stable NS bifurcation, and *two brown* curves the unstable NS bifurcation. **a** Magnified diagram of the *square* region in Fig. 5, **b** schematic of **a**

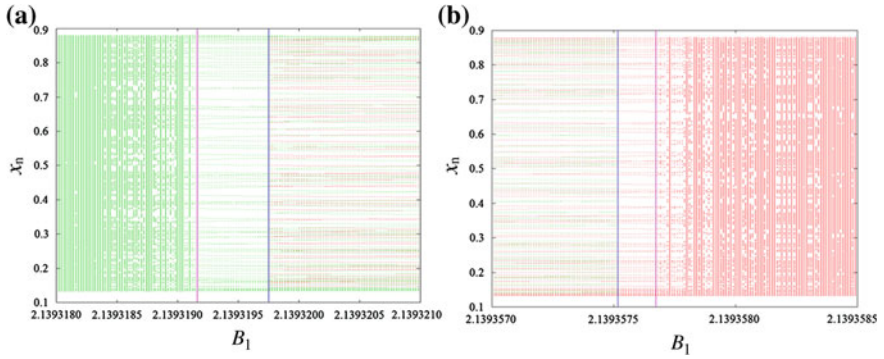

Fig. 9 One-parameter bifurcation diagrams for two solutions denoted *red* and *green* with $B_2 = 1.9825$. Other parameters are given in Fig. 3. **a** Parameter B_1 is decreased from P. The IT_0 *red* attractor disappears on the *blue line* via SN bifurcation, while the IT_0 *green* attractor gives rise to SN cycle bifurcation on the *red line* to become one-torus IT_1 attractor. **b** Parameter B_2 is increase from P. The IT_0 *green* attractor disappears on the *blue line* via SN bifurcation, while the IT_0 *red* attractor gives rise to SN cycle bifurcation on the *red line* to become one-torus IT_1 attractor

We will explain this bifurcation as follows when the parameter is changed from P to Q. At the parameter P, we obtain two coexisting periodic attractors with a period 93. When the parameter is increased across one of two skyblue curves, one of two periodic attractors presents a NS bifurcation to become IT_1, and the other one remain as IT_0. If the parameter is increased more across two skyblue curves two solutions bifurcate to become IT_1. Therefore, we observe two IT_1 as shown in Fig. 7.

Figure 9 shows a one-parameter bifurcation diagram where we use two initial points at parameter P. In Fig. 9a, we trace the two IT_0 solutions from P to the left direction. One of two periodic attractors in red disappears at SN bifurcation on the blue line. On the other hand, the periodic solution in green bifurcates to one-torus (IT_1) on the red line via a saddle-node cycle bifurcation.

In contrast, Fig. 9b shows a one-parameter bifurcation diagram where we trace the solution from P to the right. In this case, the periodic solution in green disappears at the SN bifurcation point on the blue line. Furthermore, the periodic solution in red bifurcates to one-torus (IT_1) through a saddle-node cycle bifurcation on the red line.

2 Conclusion

In this study, we investigated quasi-periodic bifurcations generated by a three-coupled delayed logistic map. We discovered two coexisting periodic solutions with period 93 in an Arnol'd tongue. By varying the bifurcation parameter to left and to right in the IT_0 Arnol'd tongue, first, a saddle-node bifurcation occurs by which one of the periodic solutions disappear, and next a saddle-node cycle bifurcation occurs through which a periodic solution bifurcates to an invariant-torus.

References

1. Broer, H., Simó, C., Vitolo, R.: The Hopf-saddle-node bifurcation for fixed points of 3D-diffeomorphisms: the Arnol'd resonance web. Bull. Belg. Math. Soc. Simon Stevin **15**, 769–787 (2008)
2. Vitolo, R., Broer, H., Simó, C.: Quasi-periodic bifurcations of invariant circles in low-dimensional dissipative dynamical systems. Regul. Chaot. Dyn. **16**, 154–184 (2011)
3. Takens, F., Wagener, F.O.O.: Resonances in skew and reducible quasi-periodic Hopf bifurcations. Nonlinearity **13**, 377–396 (2000)
4. Kuznetsov, Y.A., Meijer, H.G.E.: Remarks on interacting Neimark–Sacker bifurcations. J. Differ. Equ. Appl. **12**, 1009–1035 (2006)
5. Sekikawa, M., Inaba, N., Kamiyama, K., Aihara, K.: Three-dimensional tori and Arnold tongues. Chaos **24**, 013017 (2014)
6. Broer, H., Simó, C., Vitolo, R.: Hopf saddle-node bifurcation for fixed points of 3D-diffeomorphisms: analysis of a resonance 'bubble'. Physica D **237**, 1773–1799 (2008)
7. Shimada, I., Nagashima, T.: A numerical approach to ergodic problem of dissipative dynamical systems. Prog. Theor. Phys. **61**, 1605–1616 (1979)

http://www.springer.com/978-3-319-47808-1

Emergent Complexity from Nonlinearity, in Physics, Engineering and the Life Sciences
Proceedings of the XXIII International Conference on Nonlinear Dynamics of Electronic Systems, Como, Italy, 7-11 September 2015
Mantica, G.; Stoop, R.; Stramaglia, S. (Eds.)
2017, XXV, 222 p. 113 illus., 86 illus. in color.,
Hardcover
ISBN: 978-3-319-47808-1